

Article citation info:

Groll W, Sowiński B, Konowrocki R, Study of transitional phenomena in rail vehicle dynamics in relation to the reliability and operational state of the continuous welded rail track in terms of rail joints. *Eksploracja i Niezawodność – Maintenance and Reliability* 2023; 25(1) <http://doi.org/10.17531/ein.2023.1.7>

Study of transitional phenomena in rail vehicle dynamics in relation to the reliability and operational state of the continuous welded rail track in terms of rail joints

Indexed by:



Witold Groll^a, Bogdan Sowiński^a, Robert Konowrocki^{a,b*}

^a Railway Research Institute, 50 Chłopickiego str., 04-275 Warsaw, Poland

^b Institute of Fundamental Technological Research, Polish Academy of Sciences, 5B Pawińskiego str., 02-106 Warsaw, Poland

Highlights

- Analysis of methods of assessing the correct operational state of rail joints used in the continuous welded rail track railway lines.
- Errors in the measurement results interpretation caused by defects in classical methods of assessing the operational state of welded track joints.
- Tests of vertical vibrations of rail vehicles caused by their passage over welded track joints.
- Possibility of diagnosing the operational condition of rail joints using any type of rail vehicle.

Abstract

This paper presents the results of experimental and numerical studies on reliability and monitoring issues of railway infrastructure in terms of safety and operation. The state of knowledge concerning methods of assessing track condition, in particular rail joints used in continuous welded rail track of railway lines is described. Experimental results of rail joints used in track transition zones and the results of numerical studies/tests of the rail vehicle-track model are outlined. It is demonstrated, basing on the analyses of the experimental results, that not only should the rail joints used in continuous welded rail track be diagnosed during their acceptance, but also during their operation. It is proven that the currently used methodology for testing welded rail joints applied during acceptance testing of contact track is not fully correct and leads to misinterpretation of the measurement results. Moreover, the results of numerical simulation tests presented in this paper confirm the possibility of diagnosing the condition of rail joints by any vehicle passing over such a track equipped with a suitable system.

Keywords

operational safety, rail joint monitoring, rail vehicle dynamics, numerical and experimental studies, continuous welded rail track

This is an open access article under the CC BY license (<https://creativecommons.org/licenses/by/4.0/>)

1. Introduction

The introduction of tracks with welded rails into service has necessitated paying more attention to the workmanship in making rail joints. One of the consequences of errors in rail installation is the formation of vertical irregularities in the rail joints. This results in changes in the dynamic effects in the wheel-rail contact affecting a number of factors related to the operation of the rolling stock, degradation of the track geometry, passenger comfort, noise, etc. Inaccuracies in the rail joints, which are short disturbances in the vertical and lateral geometry of the track, generate short-term changes in the contact geometry during the passage of the rail vehicle, which can result in a change in the position of the contact point on the wheel tread and rail and in the radii of curvature of the contacting rolling surfaces. The generally different positions of the joints on the left and right rails in the track in relation to track gauge mean

that, in addition to changes in vertical geometry, local variations in cant can occur in their area. All these sudden factors can result in rail wear and local settlement, contributing to a reduction in the level of track maintenance and thus the reliability of such infrastructure. An analysis of the behaviour of the vehicle as it passes over rail joints can provide an explanation of this process.

Due to the standard length of rail sections (usually 25 m), it may occur that changes in geometry may be periodic, meaning that the rail vehicle is subject to periodic forcing while running. In general, any change in track geometry is accompanied by changes in the dynamic interaction between the vehicle and the track. As the operating speed of rail vehicles increases, these changes become more and more relevant to the long-term track behaviour [30]. The quantitative problem resulting from the number of joints and the limited number of measurement

(*) Corresponding author.

E-mail addresses:

W. Groll (ORCID: 0000-0003-0927-3411) wgroll@ikolej.pl, B. Sowiński (ORCID: 0000-0003-2956-0469), bsowinski@ikolej.pl, R. Konowrocki (ORCID: 0000-0003-1902-8030) rkonow@ippt.pan.pl

vehicles (track recording coaches – TRCs) prompt the search for solutions other than visual joint condition monitoring [17] or on-site laser measurements [2]. One such solution would be to monitor the condition of the track components through the use of so-called on-board monitoring. Quite precise practical aspects of the application of such monitoring are described in works [7,20,27,28,29,32,33]. However, it should be emphasised that in general, there have been no extensive attempts at the practical application of this type of track element condition monitoring and no focus on the identification and monitoring of track joints. In recent years, a number of studies have been carried out in many countries related to monitoring the condition of railway track geometry and investigating the quality of drive. Amongst others, the authors in [34], provided an excellent overview of the current development of such systems installed on board rail vehicles running in the UK. A detailed study carried out in Japan investigated the use of a system to measure its vertical movement mounted on the bogie frame. The system was supplemented by an additional sensor mounted on the axle-box to monitor rail geometry [37]. Furthermore, other Japanese researchers in a paper [29] proposed a track condition monitoring system using track condition classifiers, obtained by using machine learning techniques, extracted from the vibrations of the rail vehicle body passing over the diagnosed track. An approach using machine learning techniques for track condition monitoring of railway tracks was also analysed by English researchers [3]. They also identified the condition of welded joints in tracks. On the other hand, the paper [10] analysed measurements from recorded signals from multiple train passes and made conclusions about track geometry and defect location based on these. Subsequent authors in publication [1] point to the high acceleration values measured at both the bogie and the body using the car body motion detection system fitted to Acela trains fleet running in the USA. In the paper [31], concepts were developed for processing data recorded during the passage of a rail vehicle and related algorithms for monitoring track condition to improve maintenance and/or reliability. In [35], a method for monitoring the vertical irregularity of a long-wavelength track based on the acceleration of the axlebox and the inclination speed of the bogie was proposed. A comprehensive overview of track condition monitoring techniques can be found in the research report [19]. Also the railway track condition monitoring using the finite element method (FEM) is outlined in papers [4,6]. The impact of train speed on the forces of the wheelset on the track, stresses and deformations on the rail head as the wheel passes over the rail joint with a height difference between the ends of the rail joint is investigated also applying the finite element method in publication [5]. The FEM was also used in work [11], where the service life of an insulated rail joint was analysed.

In addition, extensive experimental and simulation tests of rail joints, were carried out and described in works [22,23,24] in which the influence of joint geometry on the rail-wheel interaction was investigated and the relationship between the rail joint weld irregularity gradient and the maximum dynamic wheel-rail contact forces was shown. The numerical model developed by the same author in paper [25] is used to calculate dynamic wheel-rail contact forces for a sample number of measured welded rail track joints. In the proposed approach,

general quantitative correlations between rail geometry, train speed and the level of dynamic wheel-rail contact pressure are derived. The derived statistical distributions of the geometrical properties of the rail joints and the corresponding contact forces allow an easy estimation of the level of dynamic forces occurring in the railway line based on geometrical irregularity measurements. In addition to the above techniques, the authors of the publication [36] analysed the evolution of rail weld irregularity geometry and its influence on the dynamic interaction of the wheel-rail system, both in the time and frequency domain by applying the theory of fractal geometry and a model describing the coupling dynamics of the vehicle-track system. It was found that fractal dimensions can facilitate to describe the evolution of welded rail joint irregularity geometry and its influence on the dynamic interaction of the wheel-rail system. On the other hand, papers [8,15,16] describe the results of experimental and numerical analyses of the impact of the level of the track geometry irregularity values on the dynamic interaction of forces in the wheel-rail contact area for trains and trams. Similarly, on the basis of experimental studies of the tram dynamic interaction with the track, a novel method of assessing the track condition based on the Gray Relational Analysis method was proposed in paper [26]. In the case of monitoring track components using inertial measurements during the passage of a train, the work [18] used the results of measurements from the train axle box to monitor the condition of welded joints. In this approach, the power spectrum of the acceleration signals was used as an indicator of their degradation and damage. The authors of paper [21] used a geodetic approach to detect and classify track parameters such as welded joints, crossings and turnouts.

Despite the above state of technology, it should be stressed that methods for monitoring joint geometry at the stage of their placing in service are currently mostly based on the so-called (a staff and a wedge) method described in the manual [13] and visual inspection [14]. Such techniques, due to the number of objects - joints and the route length that should be monitored, are inefficient and often fail. At the same time, the limited number of measurement vehicles and the need to ensure an adequate level of safety necessitates the need to consider monitoring the condition of the railway track by means of regularly running trains.

The aim of this article is to present a reliable, on-board monitoring-based diagnosis of the condition of the rail joint geometry of contact-free/welded track. The proposed approach deals with two aspects of the experimental study of transient phenomena associated with the passage of a rail vehicle over a rail joint of a continuous welded rail track. The geometry of the joint, as a factor generating transient interactions in the wheel-rail system, is analysed, as well as the method of its measurement and the wheel kinematics associated with the dynamic interaction between the vehicle wheel and the rail that can result in track deterioration. Moreover, joint geometry measurement techniques and their characteristic features will also be presented, with their imperfections highlighted, as well as experimental studies of the track parameters used to create a numerical model of the vehicle-rail system.

2. Track geometry measurement methods

In order to better demonstrate the problem and difficulty of identifying the operational condition of continuous welded rail track joints, it should be mentioned that each EU Member State has its own rail infrastructure manager, which is subject to standards set by the European Committee for Standardization (CEN). The standards define three levels of track geometrical quality: alarm limit (AL), intervention limit (IL) and immediate action limit (IAL). At the same time, EN 13848 [9] defines three wavelength intervals for assessing track geometry D1 (3 - 25 m), D2 (25 - 70 m), D3 (70 - 150 m). During normative studies, track geometry measurements are carried out by track recording cars (TRCs) or measurement trolleys (MTs). TRC methods are used to measure loaded track geometry (vertical irregularity) at wavelengths from 3 m (sometimes 1 m) over long distances, while MTs, designed for shorter distances and fitted with accelerometers or mechanical or laser displacement measuring systems, can measure unloaded rail irregularities for wavelengths from about 0.5 m. Although TRCs have the capability to measure short wavelengths of irregularities, filtering of the recorded data is generally applied, and this means that shorter wavelengths are eliminated from the analysed results. However, it should be stressed that from the point of view of the needs of railway companies, measurements of track geometry with a sampling frequency of approx. 0.2 m, giving the possibility of locating damage with an accuracy of approx. 5 m, are sufficient to assess, in accordance with the existing regulations concerning the operational maintenance of the track. Such accuracy is obviously insufficient for assessing the geometry of short irregularities such as rail joints.

Methods for measuring track geometry can be divided into two groups: methods related to acceptance conditions and measurement methods carried out periodically to assess changes in geometry that have occurred during track operation.

2.1 Methods of periodical track geometry measurements

Measurement vehicles (so called indirect measurement) and measurement instruments authorised for use by PKP PLK (the so-called direct measurement) are used for track geometry identification.

During the measurement, vertical track geometry parameters such as vertical track gauge irregularities, twist and cant are measured, and horizontal track geometry parameters: track gauge irregularities in the horizontal plane, gauge and gauge gradient.

Tests using measurement vehicles are carried out according to a schedule set by the relevant PKP services. The test frequency depends on the permissible maximum speeds on the railway line. In line with the Instructions for measuring, testing and assessing the condition of tracks Id-14 [12]:

1. on lines with maximum speeds $v \geq 160$ km/h - measurements are carried out 3 times a year,
2. on lines with maximum speeds of $100 \text{ km/h} \leq v < 160$ km/h measurements are carried out twice a year,
3. on lines with maximum speeds $v < 100$ km/h measurements are carried out once a year.

The EM-120 measurement trolleys are the basic vehicle used to conduct geometry measurements of track parameters under the PKP PLK responsibility. They have a rigid frame that serves

as a reference base (chord) for determining the displacements of measuring points. Under the frame, there are three two-axle measurement trolleys that also act as the vehicle's bogies. The determination of the vertical parameters values of the track geometry is carried out by measuring the displacement of the measuring wheels rolling on the rails in relation to the main frame of the vehicle (chord). The inclination of the frame in relation to the horizontal level is determined using a gyroscopic pendulum system. On the other hand, the measurement of the track geometry horizontal parameters is determined by measuring the displacement of the measuring slides guided along the inner surface of the rails in relation to the vehicle bogie frame. In the classic EM-120 measurement trolley, a contact-based method of measurement using inductive or potentiometric displacement gauges is used, while the new trolleys employ contactless systems using optical sensors. In the measurement method used for the EM120, the vertical/horizontal arrows are measured, i.e. the deviations measured from the rolling surface of the rail head to the reference line, which is a chord determined for the vertical parameters of the track geometry by two wheels of the measurement trolley distant from each other by the length of the measuring base (10 m) or, in the case of lateral parameters, by measuring slides the same distance apart. In order to determine the vertical irregularity in the case of a symmetrical chord arrangement, the resulting arrow values should be filtered by the transition function $H(\lambda)$ [9] expressed by the formula (1)

$$|H(\lambda)| = 1 - \cos\left(\pi \frac{l}{\lambda}\right) \quad (1)$$

where: l - chord length, λ - wavelength of irregularity.

Due to the shape of the transition function and the resulting transformation errors, the applied method taking into account the transition function can practically be used for a range of irregularity wave lengths from 3 m to 25 m. Accurate measurement of longer inequality wavelengths is possible with inertial systems application.

The measurement trolley measures directly such vertical and horizontal track geometry parameters as vertical right and left track arrows/irregularity, sway, cant, as well as track gauge and irregularity/ horizontal arrows. The geometric parameter signals are subjected to pre-processing, threshold analysis and synthetic analysis. As part of the pre-analysis, the secondary parameters (cant and track gauge gradient) are calculated and the mean and relative values of all parameters are calculated. The calculation of these parameters is done in increments of 0.25 m. The threshold analysis consists in comparing, depending on the track class, the values of the deviations of the track parameters with its permissible values (class A,B) or defects (class C). Synthetic analysis consists in calculating statistical parameters of the signals and, on this basis, calculating defects or synthetic indicators of track condition assessment.

Direct measurements are actually taken on short sections of track as supplementary measurements. They are carried out using electronic and laser track gauges. These devices allow measuring various geometrical parameters of the track, but due to the capacity of the batteries that power them, their operating range is limited to several kilometres. Moreover, this range is limited by the speed of the operator.

2.2 Methods of rail joint geometry measurement

The fact that the results of periodic measurements of track geometry are filtered means that defects concerning the rail joint geometry created during operation are inaccessible to the services diagnosing railway infrastructure and, in practice, the assessment of the condition of the joint is reduced to its visual inspection. The acceptance conditions for a thermite-welded joint are specified in the Railway Welding Manual [13]. This manual shows that the joint geometry is checked by testing its straightness using an electronic staff with computer recording with a measurement base of 1 m length and accuracy of minimum 0.02 mm for tracks with speed $v > 160$ km/h, or a steel staff of 1 m length (Fig. 1), measuring wedges (gap gauge - the so-called "staff and a wedge" method). The steel staff is used both to align the rail ends and to check the straightness of rail joints with a measurement accuracy of at least 0.05 mm for tracks with a speed $v \leq 160$ km/h. However, for tracks with speed $v > 160$ km/h, in addition to the above, the cross-sectional measurement should be carried out with a profile gauge in the joint axis and on both sides at a distance of 250 mm. The permissible geometrical deviations of the rail joint are shown in Table 1.

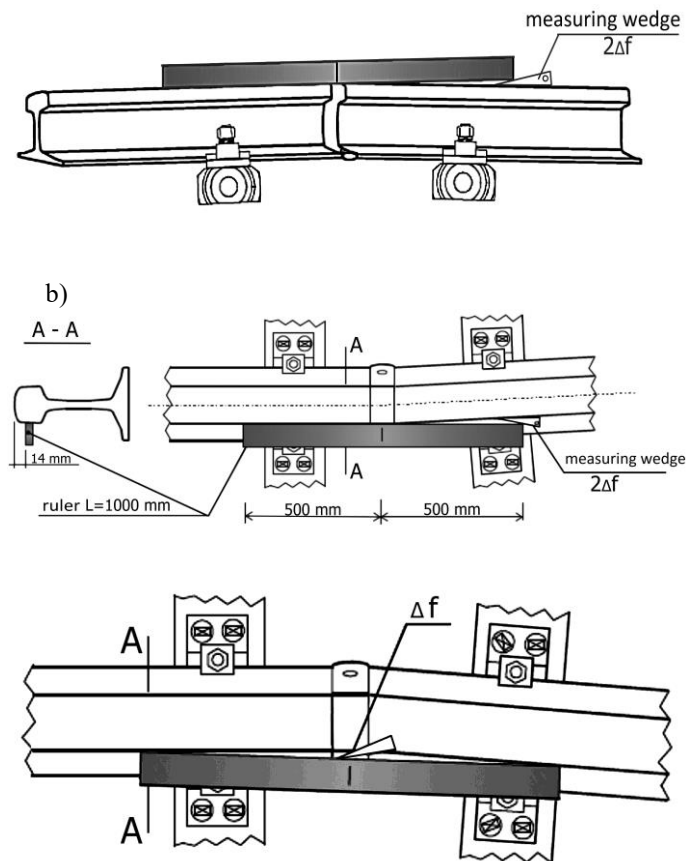
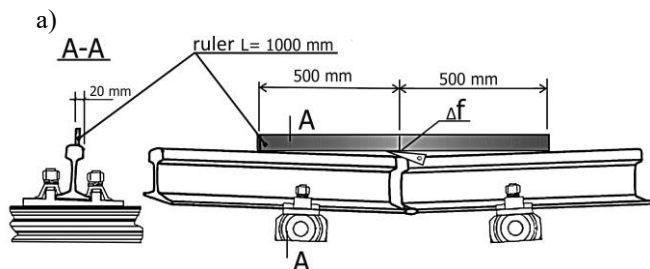


Fig. 1. Method of measuring weld geometry with a steel staff used at the acceptance stage and method of assessing joint condition [13], (a) vertical irregularity, (b) lateral irregularity.

Table 1. Permissible deviations in the rail joint geometry [13] permissible vertical straightness deviations.

type of defect and its classification	dimensional deviations Δf [mm]					
	main tracks				remaining tracks	
	$V > 160$ km/h		$V \leq 160$ km/h			
	convexity	concavity	convexity	concavity	convexity	concavity
absence of defect	$\Delta f \leq 0,3$	$\Delta f = 0$	$\Delta f \leq 0,3$	$\Delta f \leq 0,1$	$\Delta f \leq 0,5$	$\Delta f \leq 0,5$
defect to be repaired	$0,3 < \Delta f \leq 0,5$	$0 < \Delta f \leq 0,2$	$0,3 < \Delta f \leq 0,5$	$0,1 < \Delta f \leq 0,3$	$0,5 < \Delta f \leq 1,0$	$0,5 < \Delta f \leq 0,8$
defect requires to be cut out	$\Delta f > 0,5$	$\Delta f > 0,2$	$\Delta f > 0,5$	$\Delta f > 0,3$	$\Delta f > 1,0$	$\Delta f > 0,8$
type of defect and its classification	permissible deviations of horizontal straightness Δf [mm]					
	main tracks				remaining tracks	
	convexity		concavity			
absence of defect	$\Delta f = 0$		$\Delta f \leq 0,3$		$\Delta f \leq 0,5$	$\Delta f \leq 0,5$
defect to be repaired	$0 < \Delta f \leq 0,3$		$0,3 < \Delta f \leq 0,6$		$0,5 < \Delta f \leq 0,8$	$0,5 < \Delta f \leq 0,8$
defect requires to be cut out	$\Delta f > 0,3$		$\Delta f > 0,6$		$\Delta f > 0,8$	$\Delta f > 0,8$

The method of measurements a track profile using a staff and wedge' device is extremely burdensome and time-consuming. The use of a profilometer eliminates these difficulties and significantly increases the accuracy of the survey compared to other measurement methods.

Older profilometers are mechanical devices in which the movement of the measuring head is guided manually along a guide based on the surface of the rail, and measurement is based on the reading of a dial gauge. More modern devices of this type include mechanical-electronic profilometers, in which the rail still has to be manually contoured, however, the reading is recorded digitally, or optical-electronic profilometers, where measurement takes place fully automatically, due to the use of laser scanning technology.

The joint geometry measurements discussed in this article were carried out using the PRS02W laser profilometer owned by the Railway Research Institute, the parameters of which are summarised in Table 2. The measurement process with this device is fully automatic. The use of a laser optical sensor with a prism in this device allows measurement in a plane parallel to the sensor. This functionality also allows measuring the profile of rails in turnouts.

Table 2. Metrological characteristics of the laser profilometer.

parameters	values
range of irregularity measured	+/- 5 mm
resolution	10 μm
measurement base	1000 mm
scanning range	1038 mm
scanning resolution	1 mm
vertical measurement line from the rail side surface	20 mm
horizontal measurement line below rolling surface	14 mm



Fig. 2. PRS02W laser profilometer used for tests.

It should be noted that a profilometer measurement provides a better representation of the joint geometry than a steel staff measurement. Measurement with a steel staff determines, in the case of a dipped rail joint, its maximum amplitude of irregularity and, in the case of a peaked rail joint, the irregularity gradient.

2.3 Results of joint geometry measurements

As part of the experimental measurements of the geometry of the contact track rail joints under consideration, more than one hundred rail joints were analysed on tracks of varying technical

condition. Measurements of rail joints were carried out on sections of track with UIC60-type rails at a track gauge of 1.435 m and a rail inclination of 1:40. The length of the measured track section for each joint was 1,000 mm, with a recording frequency of 0.5 cm. The results of the measurements showed that the condition of the joints geometry had deteriorated significantly over the course of the track. The dimensions of the joints (Fig. 3) significantly exceeded the permissible dimensions indicated in Table 1.

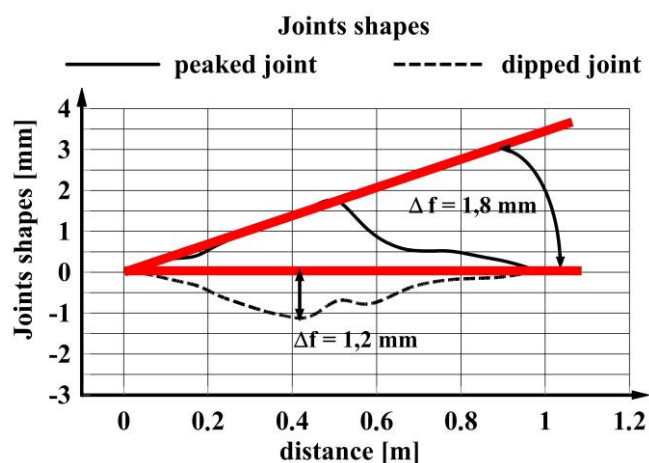


Fig. 3. Examples of vertical rail irregularity of measured joints with extreme dimensions.

The range of change in the irregularity amplitude was between -1.2 mm and 1.8 mm, the change in the gradient was between -0.012 and 0.012, and the curvatures were between -0.5 $1/m$ and 0.4 $1/m$. The standard deviation of the joint irregularity varied between 0.04 mm and 0.5 mm. It should also be noted that, among the joints measured, there were some that could not be unambiguously classified as hollow (dipped) or curved (peaked).

In order to make a partial assessment of the condition of the joints located on the Żmigród track, measurements were made of the irregularities occurring in their 1 metre zones, and selected examples are shown in Figure 4. A total of 50 joints on both rail tracks were measured. Vertical irregularities were measured at 20 mm from the top of the rail head of the left and right rail tracks, and lateral irregularities were measured at 14 mm below the top of the rail head on the centreline side of the track, this allowed the change in width to be determined and allowed estimating the curvature of the rail in the case of a non-central set position.

Examples of rails joints vertical and lateral irregularities

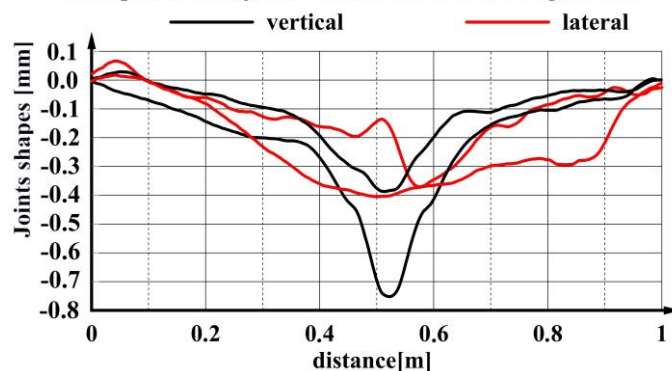


Fig. 4. Examples of vertical and lateral irregularities in the rail joint zone.

The analysis of the measured irregularities (amplitudes and gradient) allows hypothesising that the irregularities in the joint zone on the test track in Żmigród are smaller than those observed on railway lines in normal operation. In the case of the test track, the range of changes in the amplitudes of the irregularities did not exceed 0.75 mm, while it was 1.8 mm in the case of the track under normal operation. Also in the case of the analysis of the gradient of changes in irregularities, its smaller values were found for the test track. Among the measured irregularities, those to be classified as dipped predominated

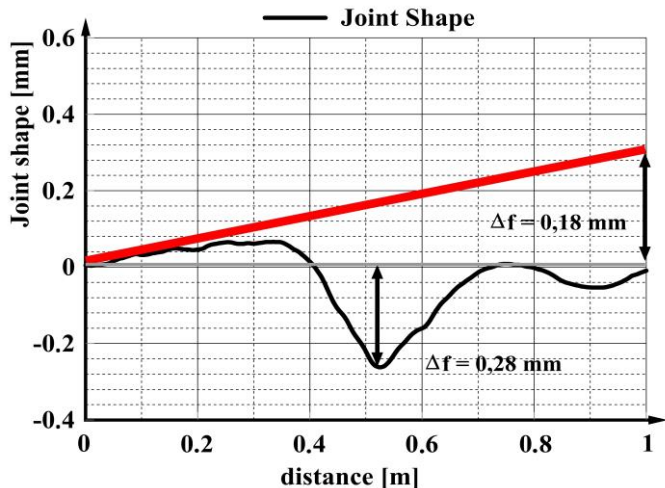


Fig. 5. A joint including the features of a dipped and peaked rail joint.

It should be noted that, according to the classification of joint shape into dipped and peaked, only one of the joints analysed by the authors of this paper can be unambiguously classified as dipped. The other joints bear the characteristics of dipped and peaked rail joints (Fig. 5), and according to the measurement method presented in Manual Id-5 [13], they would be classified as peaked. The use of such a method of identifying rail joints, can cause misinterpretation of the results obtained. For instance, the deviation in geometry of the joint (Fig. 5), while classifying it as peakedity, according to the Manual should be treated as acceptable for main tracks operated at speeds $v > 160$ km/h. However, treating this joint as dipped would qualify it for repair. This leads to a very high degree of ambiguity in the results of the measurement of welded joints of contact track using the method described, and thus their correct qualification.

Due to the location of the tested joints at the entrance to the curve, five measurements of the rail profiles before and after welding were taken near each joint every 30 cm on the right and left rails. The measurements showed no significant wear on the profiles.

3. Measurement of the wheelset accelerations

The next stage of the experimental investigations carried out to analyse the rail joints mentioned in the paper was their indirect measurement performed on the components of vehicle during the ride over them. In this case, accelerations were measured on the wheelset bearing cases. Measurements of the vertical acceleration of the left and right wheels, as well as the lateral acceleration of the wheelset, were carried out for two types of vehicle: a four-car multiple unit, and a three-car multiple unit, for which the axle load was approximately 160 kN and 180 kN respectively.

Accelerometers measuring the acceleration of the vehicle components were placed on the carbody, bogie frame and wheelsets. A section of track was selected for these tests, in which there were five consecutive rail joints on the left rail track at the start of the transition curve entrance. However, the location of the joints on the right rail track, of the selected track section, was moved from the joints on the left rail track between 2 m and 4 m. The geometry of these joints was identified and their vertical profiles are shown in Figure 6.

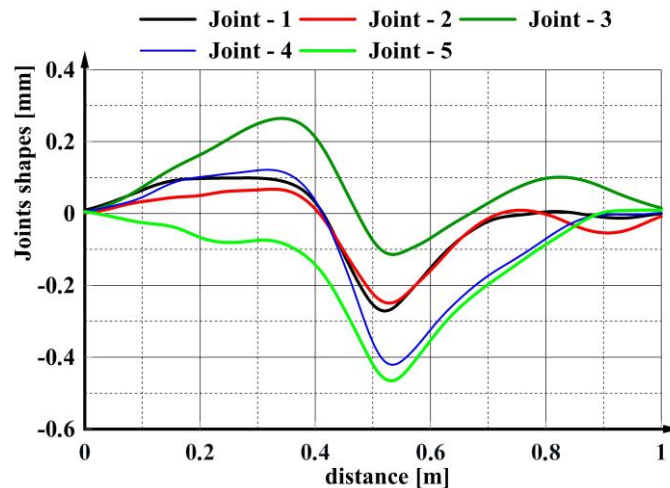
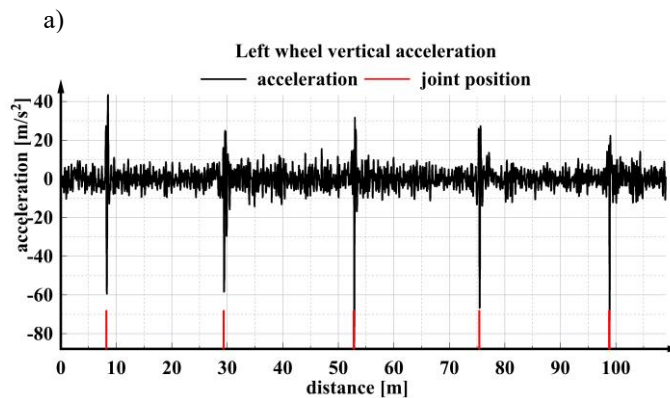


Fig. 6. Vertical joint profiles measured on the test track section.

During the tests, five runs were made with the sensor-fitted vehicle on the test track at speeds of 80, 100, 120 and 140 km/h. The vertical and lateral accelerations of the wheelset were measured for a four-carriages vehicle, and the vertical accelerations of the wheelset were measured for a three-carriages vehicle. The vertical and horizontal acceleration was measured using an accelerometer mounted on the wheelset bearing case. The sampling frequency of the acceleration signal was 2400 Hz for the four-member vehicle and 300 Hz for the three-car vehicle. Photocells were placed at the track locations of the selected joints to identify the moment when the wheelset passed the joint.

Examples of measurements of the vertical acceleration of the left and right wheels and the lateral acceleration of the wheelset are shown in the diagrams (Fig. 7). These measurements were taken during the passage of a four-car trainset running at approximately 100 km/h.



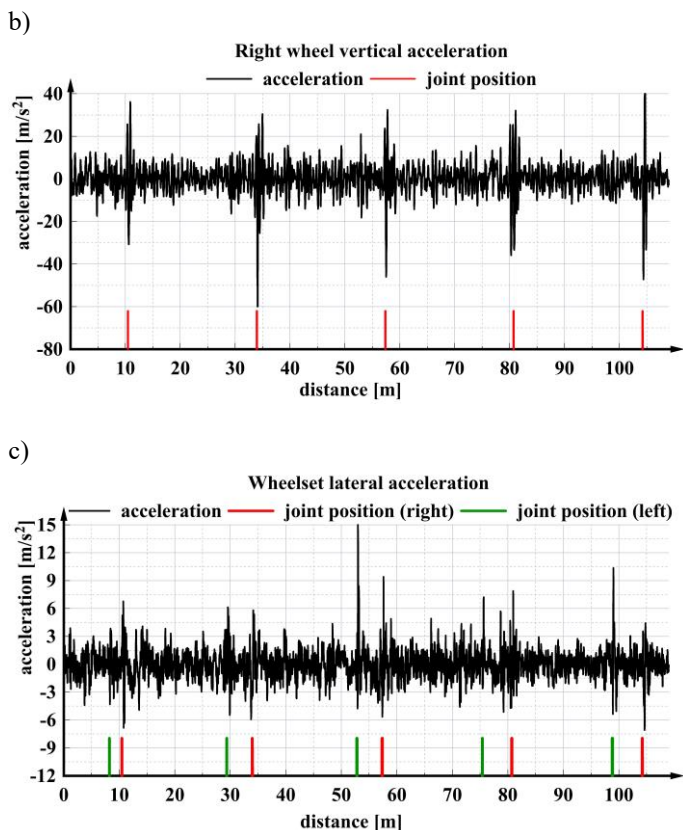


Fig. 7. Vertical acceleration of the bearing case of (a) the left and (b) the right wheels of a wheelset and (c) the lateral acceleration of this wheel-set.

The results of the measurements were highly repeatable and showed, the occurrence of periodic, rapid changes in the vertical acceleration of the wheel. The distance between the recorded changes was about 25 m, which corresponds to the distance between the rail joints identified in the test track. Also, measurements made for a three-car vehicle performed at a lower sampling frequency showed periodic effects of joint geometry on the vehicle (Fig. 8). From the measurements obtained, we can conclude that also in the range of lower sampling frequencies, the effect of passing over the joints on the kinematics of the set is observed.

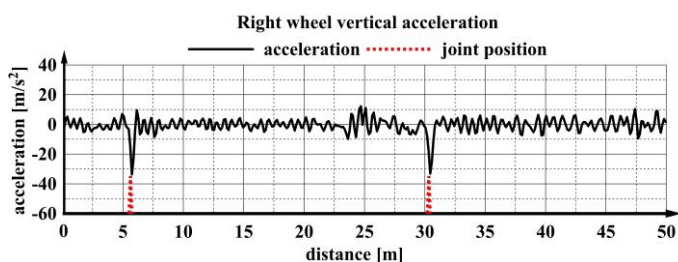


Fig. 8. Vertical acceleration of the right wheel of a three-car vehicle.

The extreme values of the accelerations recorded during the performed passing over the rail joints on the Żmigród track is included in Table 3.

Table 3 Extreme acceleration values recorded during all test drives.

speed [km/h]	left wheel vertical acceleration range from - to [m/s ²]	right wheel vertical acceleration range from - to [m/s ²]	wheelset lateral acceleration range from - to [m/s ²]
80	-65 ÷ 33	-35 ÷ 32	-10 ÷ 12
100	-92 ÷ 41	-53 ÷ 62	-15 ÷ 16
120	-106 ÷ 51	-76 ÷ 73	-16 ÷ 15
140	-112 ÷ 63	-106 ÷ 87	-16 ÷ 16

Table 3 data show that the range of changes in vertical wheel acceleration increases with increasing vehicle speed. These changes are evident on both rail tracks. However, it should be noted that the lateral accelerations of the wheelset hardly changed with increasing speed.

An example of the effect of vehicle speed on the recorded changes in wheel accelerations in the marked area of the joint zone is shown in Fig. 9. The measurements were made for a four-car vehicle. The analysis of the vertical wheel accelerations (Fig. 9) shows that, in certain cases, increasing the speed from 80 km/h to 140 km/h can cause a significant change in the vertical acceleration values.

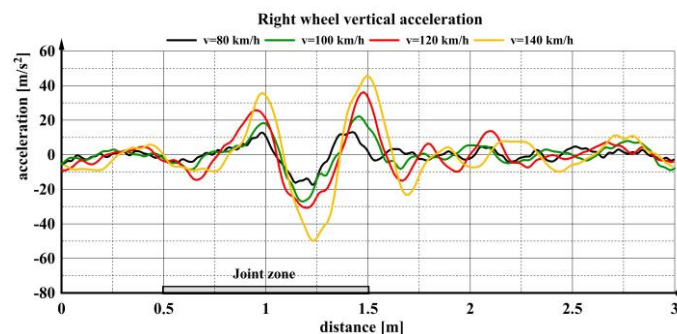


Fig. 9. Impact of vehicle speed on recorded vertical wheel acceleration values.

4. Track vertical stiffness tests

In addition to the tests described above, an experimental analysis of the effect of the joint weld presence on the track parameters was also carried out. It is worth noting that the joint weld, in addition to the kinematic disturbance of vehicle movement, is also an element that introduces an anomaly in the continuity of the material structure of the rail. This causes a change in its mechanical properties. The most significant of these is the change in vertical stiffness of the track, which causes an increase in deflection of the rail, altering the kinematics and dynamics of the passing rail vehicle.

The stiffness measurements considered were carried out at two locations, i.e. at the joint and at a distance of 10 m from it. The deflection of the rail (Fig. 10) under a passing vehicle was recorded using a camera at 100 frames/sec.

a)



b)



Fig. 10. Views of analysed track sections a) tested weld, b) rail deflection measurement without weld.

In this case, other rail vehicles were used for the tests, with axle loads of 150 kN and 200 kN respectively. The vehicles were running at low speed, that eliminated the dynamic effects between wheels and rails. The measurement results showed the impact of the joint on the change in vertical stiffness of the track. The stiffness changes were characterised by a large range of $5 \cdot 10^7$ N/m to $7 \cdot 10^7$ N/m.

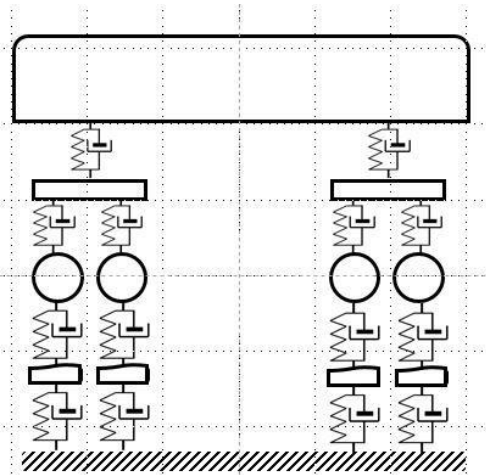
5. Simulation tests

Simulation tests were carried out for several rail vehicle models. Their aim was to determine whether the kinematic effects associated with passing over joints occur independently of the type of car. The simulation tests were carried out on a straight track with a length of several hundred metres. There were rail joints on the left rail track at distances of 25 m from the starting point of the vehicle movement. The right rail track was free of irregularity. The movement of the vehicle models was investigated for speeds varying from 50 km/h to 250 km/h.

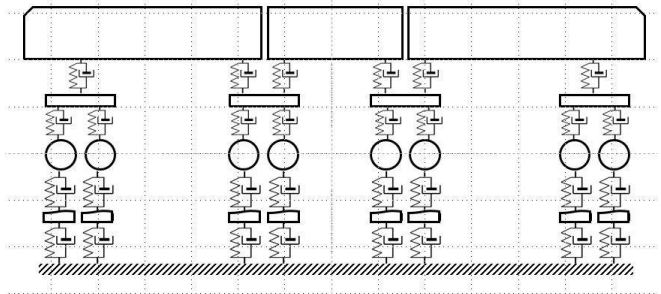
5.1 Description of vehicle models

In order to study the response of a rail vehicle to a rail joint crossing, three mathematical vehicle models were built: a four-car model, a three-car model and a model of a typical passenger car. The physical vehicle models considered in this article are shown schematically in Figure 11.

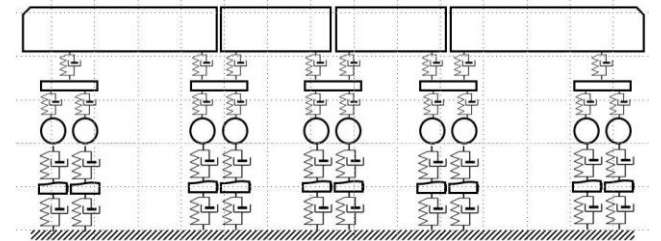
a)



b)



c)



d)

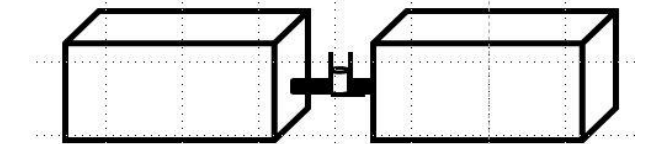


Fig. 11. Topology of the physical models of the test vehicles (a) a typical passenger car, a three-car vehicle, a four-car vehicle and a connector model between the car body blocks.

In all the models studied, they were assumed to consist of rigid bodies representing the car bodies, bogie frames (with the conventional inclusion of other parts rigidly attached to them as frames) and wheelsets. The bogies, in the case of the model of a typical passenger car, are of conventional construction, in which the wheelsets are connected to the rigid frame by a system of springs and dampers that form the first suspension stage. Each bogie has a central pivot that allows the bogie to rotate on curves and transfer longitudinal force between the bogies and the car body.

In the case of multi-car vehicle models, Jakobs bogie models were introduced, where the pin that allows the bogie to rotate is connected to the connector between the car body blocks. Furthermore, in this case, the number of spring-damper elements between the bogie frame and the car body blocks was increased. The first- and secondary suspension elements were assumed to be massless and, with the exception of the bumpers, to have linear stiffness and damping characteristics.

In the primary suspension system, the vertical spring systems were modelled as single springs and placed at the ends of the wheel sets. They were assumed to have a high compression/extension stiffness ratio to support the car body and bogie frame. A system of lateral and longitudinal springs was introduced into the model, positioned like the vertical springs. These springs realise the shear of the vertical springs of the real object in the model. The values of the stiffness coefficients of the lateral springs compared to the vertical springs are smaller, allowing lateral movements of the wheelset. A high value for the stiffness coefficient of the longitudinal springs was adopted in order to limit the torque (about the vertical axis) of the wheelset relative

to the bogie frame. The vibration damper systems were assumed to be parallel to the springs and placed in an identical orientation to the spring systems. Vertical and lateral bumpers with non-linear progressive stiffness characteristics were introduced in the primary suspension model. As in the primary suspension system, the springs and dampers of the secondary suspension were adopted as spring-damper elements connected in parallel with linear characteristics.

The bogie frames are equipped with two arrangements of springs and dampers located on their edges. Analogous to the primary suspension, lateral and longitudinal springs and corresponding damping elements were introduced into the model.

The mathematical model of a vehicle running on a track contains two cooperating subsystems, namely a train model and a track model. For the study of vertical dynamics, the track was assumed to be a susceptible element (Fig. 12). In the vehicle model, essentially dedicated to higher vibration frequencies, a Hertzian spring was placed between the wheel and the rail. When studying the lateral dynamics of the system, the track was assumed as a rigid element.

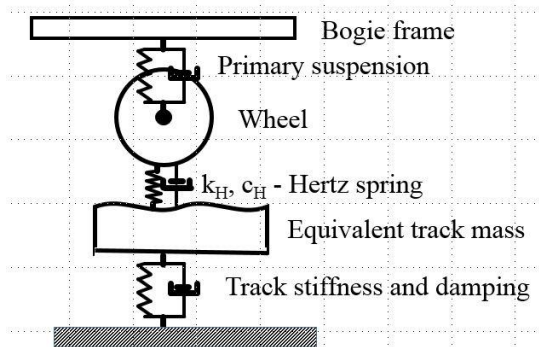


Fig.12. Wheel-rail contact model

The vertical force between the wheel and the rail V_{wr} was calculated based on the non-linear Hertz theory (2).

$$V_{wr} = \begin{cases} k_H (z_{wL,R}(t) - z_{rL,R}(t) - z_{L,R}(t))^{\frac{3}{2}} + c_H (\dot{z}_{wL,R}(t) - \dot{z}_{rL,R}(t) - \dot{z}_{L,R}(t)) & \text{if } z_{wL,R}(t) - z_{rL,R}(t) - z_{L,R}(t) > 0 \\ 0 & \text{if } (z_{wL,R}(t) - z_{rL,R}(t) - z_{L,R}(t)) \leq 0 \end{cases} \quad (2)$$

where: $z_{wL,R}$, $z_{rL,R}$, $z_{L,R}$ – vertical displacement of the wheel (left L, right R), rail (left and right) and vertical irregularity on the left and right rails respectively, c_H – damping coefficient, k_H – Hertz stiffness coefficient - dependent on the radii of curvature of the contacting blocks, the pressure on the blocks and the material parameters of the blocks.

$$k_H = \frac{2G}{3(1-\nu)} \sqrt{2 * R_e}; R_e = \frac{2r_s r_w}{r_s + r_w}; G = \frac{E}{2(1+\nu)} \quad (3)$$

where: G - shear modulus, E - modulus of elasticity; r_s and r_w - radii of curvature of the rail and wheel, ν - Poisson's ratio.

Parameters corresponding to the geometrical point of contact between wheel and rail at the central position of the wheel set are taken as radii of curvature. When modelling the wheel-rail contact through the Hertz spring, the fact that it does not act in tension was taken into account.

An inertial element with one degree of freedom modelling the vertical movement of the track is connected with each car wheel. The mass of this element is the equivalent mass of the

rails and sleepers treated together, and the elastic-damping parameters are linear with values corresponding to the mechanical parameters of the ballast: i.e. track stiffness $7e7$ N/m damping $1e5$ Ns/m, equivalent mass of the rail track 200 kg.

5.2 Verification of numerical models

In verifying the mathematical models due to the completely unknown initial conditions of the vehicle's movement, prior to entering the joint zone, it was limited to comparing the experimental acceleration values recorded during the passage over the joints and the values obtained from the simulation model. The results shown here refer to a comparison of the accelerations of the four-car model and the results obtained from the experimental measurements. A comparison of these figures at vehicle speeds of 80 and 100 km/h is shown in Figure 13.

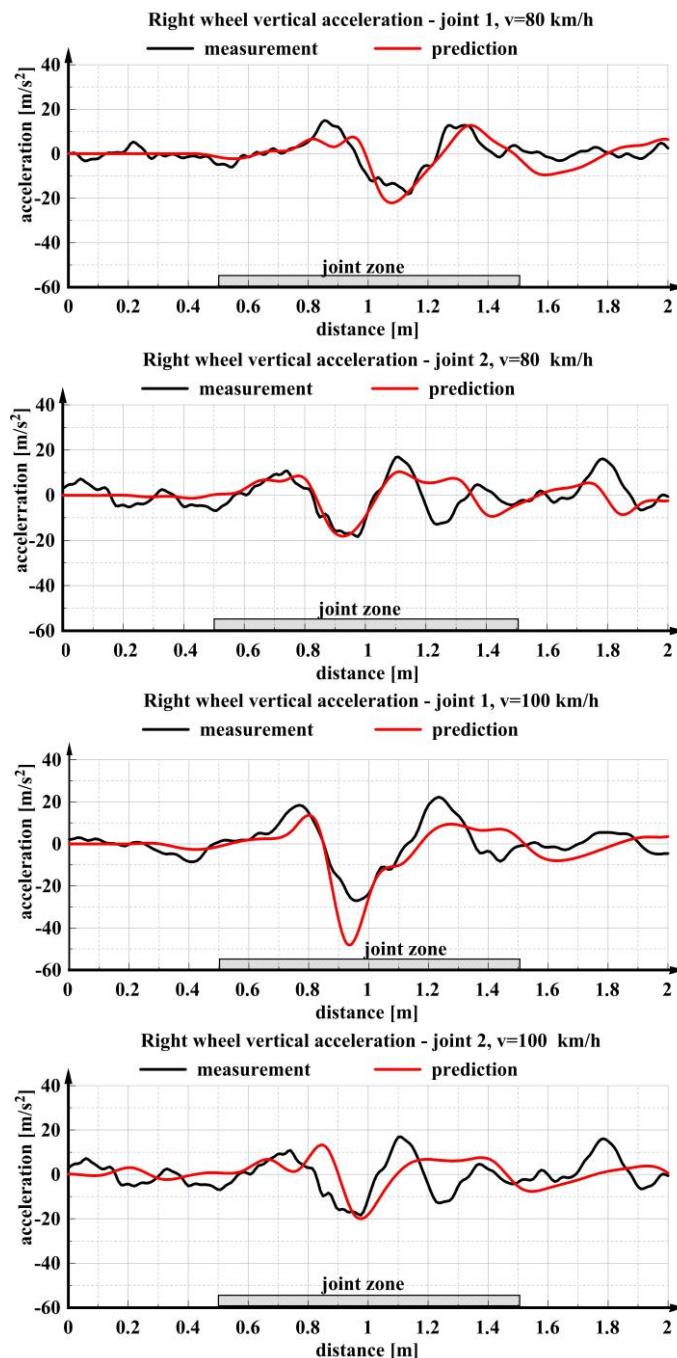


Fig. 13. Comparison of numerical simulation results with experimental trackside measurements.

The model illustrates well the locations of the extreme acceleration values and their qualitative nature. The Pearson correlation coefficient between the simulation and measurement results is close to 0.7 in all cases. The average difference between the measurement value and the simulation result for successive wheel positions in the joint zone is about 11 m/s² not exceeding 15% of the maximum acceleration values obtained from measurements, and the Fréchet distance is about 19.5 m/s². Analysis of the results obtained from the simulation studies shows that the models built also reflect well the periodicity of the joint occurrence (Fig. 14).

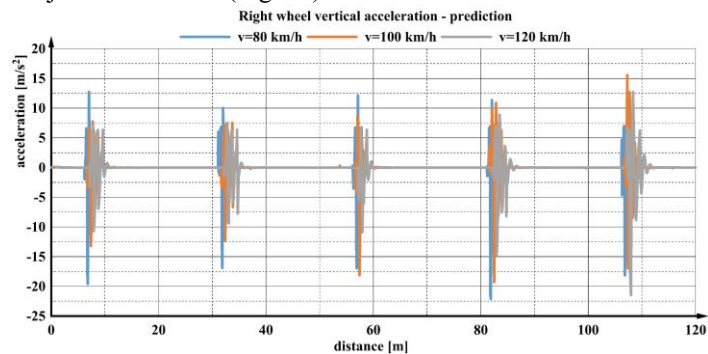


Fig. 14. Simulation results showing periodicity of rails joints.

On the basis of the results obtained from the simulation studies, it can be hypothesised that the measurement of wheelset accelerations using inertial sensors such as accelerometers or gyroscopes gives information about the condition of the rail joints on the track sections under study. It should also be stressed that monitoring the condition of the on-board joints is largely independent of the type of vehicle on which the accelerations are measured.

5. Conclusions

The idea of monitoring the condition of rail joints (welded joints) using wheel set acceleration measurements is discussed in this article considers. Short geometrical irregularities cause impulsive impacts on the vehicle and the occurrence of relevant interaction forces on the rail track. This consequently contributes to the formation and increase of geometric vertical track irregularities. Monitoring the condition of the joints is particularly important on routes where trains are operated at speeds higher than 160 km/h. As experiments have shown, an increase in vehicle speed causes a significant increase in vertical accelerations. Analysis of the currently used visual inspection method of assessing the quality of rail joints has shown that it can lead to misinterpretations of their geometry. It seems more appropriate to analyse their kinematic interactions with the rail vehicle in order to identify their condition.

Field tests were conducted on the test track of the Railway Research Institute in Żmigród for two types of rail vehicles running at different speeds. The vehicles were equipped with accelerometers fitted, among others, on the wheel-set bearing housings. Simulation studies have shown that, also for typical passenger railcars, passing over rail joints where the geometry has deteriorated due to its use causes an increase in vertical wheel acceleration values.

The method of monitoring the joints condition by measurement on vehicles equipped with suitable sensors, combined with GPS positioning, is considerably cheaper than using specialised measurement vehicles (TRCs). Field tests have shown that inertial sensors are sufficient for this purpose. They are characterised by simplicity, low cost and efficiency and can be installed on the axle-box, bogie or inside the rail vehicle. This method of diagnosing track condition does not disrupt the rhythm of trains running on the route, and also allows identifying and locating the occurrence of track defects such as squatting or buckling.

References

1. Ackroyd P, Angelo S, Nejtkovsky B, Stevens J. Remote ride quality monitoring of Acela train set performance, ASME/IEEE Joint Rail Conference, Washington, DC, USA 2002;171–178, <https://doi.org/10.1109/RRCON.2002.1000109>.
2. Aniszewicz A, Mariusz Fabijański M. Measurements of railway welded rail joints with a laser device, *Welding Technology Review*, 2020; 92(6):37-43, <https://doi.org/10.26628/wtr.v92i6.1118>.
3. Brant J, Liang B. Condition monitoring systems in the railway industry. In *advances in asset management and condition monitoring*. Smart Innovation, Systems and Technologies; Ball, A., Gelman, L., Rao, B., Eds.; Springer: Cham, Switzerland, 2020; 166:671-683, https://doi.org/10.1007/978-3-030-57745-2_56.
4. Bruni S, Goodall R., Mei T. X., Tsunashima H. Control and monitoring for railway vehicle dynamics, *Vehicle System Dynamics* 2007; 45:743-779, <https://doi.org/10.1080/00423110701426690>.
5. Cai, Wen Z, Jin S, Zhai W., Dynamic stress analysis of rail joint with height difference defect using finite element method, *Engineering Failure Analysis* 2007; 14:1488–1499, <https://doi.org/10.1016/j.engfailanal.2007.01.007>.
6. Charles, G., Goodall, R., Dixon, R. Model-based condition monitoring at the wheel–rail interface, *Vehicle System Dynamics*, 2008; 46(1):415–430, <https://doi.org/10.1080/00423110801979259>.
7. Chudzikiewicz A, Bogacz R, Kostrzewski M, Konowrocki R. Condition monitoring of railway track systems by using acceleration signals on wheelset axle-boxes. *Transport* 2018; 33(2):555-566, <https://doi.org/10.3846/16484142.2017.1342101>
8. Chudzikiewicz A, Korzeb J. Simulation study of wheels wear in low-floor tram with independently rotating wheels. *Archive of Applied Mechanics* 2018; 88: 175–192, <https://doi.org/10.1007/s00419-017-1301-6>.
9. EN 13848-1:2019 Railway applications - Track - Track geometry quality - Part 1: Characterization of track geometry.
10. Heirich O, Lehner A, Robertson P, Strang T. Measurement and analysis of train motion and railway track characteristics with inertial sensors, 14th International IEEE Conference on Intelligent Transportation Systems (ITSC) 2011, <https://doi.org/10.1109/ITSC.2011.6082908>.
11. Himebaugh AK, Plaut RH, Dillard DA. Finite element analysis of bonded insulated rail joints, *International Journal of Adhesion and Adhesives* 2008; 28:142–150, <https://doi.org/10.1016/j.ijadhadh.2007.09.003>.
12. Instructions for measuring, testing and assessing the condition of tracks/Instrukcja o dokonywaniu pomiarów, badań i oceny stanu torów Id-14, Instrukcje PKP Polskie Linie Kolejowe S.A. (in Polish)
13. Instructions for welding rails with termite/Instrukcja spawania szyn termitem Id-5, Instrukcje PKP Polskie Linie Kolejowe S.A. (in Polish).

14. Judek S, Skibicki J. Visual method for detecting critical damage in railway contact strips, *Measurement Science & Technology*, 2018; 29(5):1-8, <http://dx.doi.org/10.1088/1361-6501/aaa9af>.
15. Konowrocki R, Chojnacki A. Analysis of rail vehicles' operational reliability in the aspect of safety against derailment based on various methods of determining the assessment criterion. *Eksploatacja i Niezawodność - Maintenance and Reliability* 2020; 22(1):73-85, <http://dx.doi.org/10.17531/ein.2020.1.9>.
16. Konowrocki R, Kalinowski D, Szolc T, Marczewski A. Identification of safety hazards and operating conditions of the low-floor tram with independently rotating wheels with various drive control configurations, *Eksploatacja i Niezawodność - Maintenance and Reliability* 2021; 23(1):21-33, <http://dx.doi.org/10.17531/ein.2021.1.3>.
17. Liu Y, Sun X, Hock J, Pang J. A YOLOv3-based deep learning application research for condition monitoring of rail thermite welded joints, *IVSP '20: Proceedings of the 2020 2nd International Conference on Image, Video and Signal Processing*, 2020; 33-38, <https://doi.org/10.1145/3388818.3388827>.
18. Molodova M, Oregui M, Núñez A, Li Z, Dollevoet R. Health condition monitoring of insulated joints based on axle box acceleration measurements. *Engineering Structures* 2016; 123:225–235, <https://doi.org/10.1016/j.engstruct.2016.05.018>.
19. Nielsen J, Berggren E, Lölgen T, Müller R, Stallaert B., Pesqueux L. Overview of methods for measurement of track irregularities important for ground-borne vibration, *UIC Collaborative Project Report*, Rivas, Nicaragua, SCP0-GA-2010-265754, 2013.
20. Roberts C, Weston P, Ling CS, Goodman C. New methods for track monitoring. *IEEE seminar on Railway Condition Monitoring, Ref. No. 2004/10513*, 2004; 64-78. <https://doi.org/10.1049/ic:20040167>
21. Salvador P, Naranjo V, Insa R, Teixeira P. Axlebox accelerations: Their acquisition and time-frequency characterisation for railway track monitoring purposes. *Measurement* 2016; 82:301–312 <https://doi.org/10.1016/j.measurement.2016.01.012>.
22. Steenbergen MJMM, Esveld C. Rail weld geometry and assessment concepts. *Proceedings of the Institution of Mechanical Engineers, Part F: Journal of Rail and Rapid Transit*, 2006; 220: 257-271, <https://doi.org/10.1243/09544097JRRT38>.
23. Steenbergen MJMM, Esveld C. Relation between the geometry of rail welds and the dynamic wheel–rail response: numerical simulations for measured welds. *Proceedings of the Institution of Mechanical Engineers, Part F: Journal of Rail and Rapid Transit*, 2006; 220:409-423, <https://doi.org/10.1243/09544097JRRT87>.
24. Steenbergen MJMM. Modelling of wheels and rail discontinuities in dynamic wheel–rail contact analysis, *Vehicle System Dynamics* 2006; 44(10):763-787, <https://doi.org/10.1080/00423110600648535>.
25. Steenbergen MJMM. Quantification of dynamic wheel–rail contact forces at short rail irregularities and application to measured rail welds, *Journal of Sound and Vibration* 2008; 312:606–629, <https://doi.org/10.1016/j.jsv.2007.11.004>.
26. Tabaszewski M, Firlík B. Assessment of the track condition using the Gray Relational Analysis method, *Eksploatacja i Niezawodność - Maintenance and Reliability* 2018; 20(1):147-152, <http://dx.doi.org/10.17531/ein.2018.1.19>
27. Tsunashima H, Naganuma Y, Kobayashi T. Track geometry estimation from car-body vibration. *Vehicle System Dynamics* 2014; 52(Sup1):207–219, <https://doi.org/10.1080/00423114.2014.889836>.
28. Tsunashima H, Naganuma Y, Matsumoto A, Mizuma T, Mori H. Condition monitoring of railway track using in-service vehicle. In: Perpinya X, editor. *Reliability and safety in railway*. InTech, 2012; 333-356, ISBN978-953-51-0451-3, <https://doi.org/10.5772/35205>
29. Tsunashima H. Condition monitoring of railway tracks from car-body vibration using a machine learning technique. *Applied Sciences* 2019; 9:2734, <https://doi.org/10.3390/app9132734>.
30. Tzanakakis K. The railway track and its long term behaviour: A handbook for a railway track of high quality, Tom 2, *Springer Tracts on Transportation and Traffic*, Springer Science & Business Media, 2013; 414, ISBN 3642360513. <https://doi.org/10.1007/978-3-642-36051-0>
31. Ward, C. P., Weston, P. F., Stewart, E. J. C., Li, H., Goodall, R. M., Roberts, C., Mei, T. X., Charles, G., Dixon, R. Condition Monitoring Opportunities Using Vehicle-Based Sensors, *Proceedings of the Institution of Mechanical Engineers, Part F: Journal of Rail and Rapid Transit* 2011; 225(2):202–218, <https://doi.org/10.1177/09544097JRRT406>.
32. Weston PF, Ling CS, Goodman CJ, Roberts C, Li P, Goodall RM. Monitoring vertical track irregularity from in-service railway vehicles. *IMEchE Pt F: J Rail Rapid Transit*. 2007; 221(1):75-88, <https://doi.org/10.1243/09544097JRRT65>.
33. Weston PF, Ling CS, Goodman CJ, Roberts C, Li P, Goodall RM. Monitoring lateral track irregularity from in-service railway vehicles. *IMEchE Pt F: J Rail Rapid Transit* 2007; 221(1):89-100, <https://doi.org/10.1243/09544097JRRT64>.
34. Weston, P. F., Roberts, C., Yeo, G., Stewart, E. Perspectives on railway track geometry condition monitoring from in-service railway vehicles, *Vehicle System Dynamics: International Journal of Vehicle Mechanics and Mobility* 2015; 53(7):1063–1091, <https://doi.org/10.1080/00423114.2015.1034730>.
35. Xing Z, Chen Y, Qing Y. On-line monitoring of vertical long wavelength track irregularities using bogie pitch rate, *Journal of Vibroengineering* 2015; 17(1):216–228.
36. Xu J, Wang P, Gao Y, Chen J, Chen R. Geometry evolution of rail weld irregularity and the effect on wheel-rail dynamic interaction in heavy haul railways. *Engineering Failure Analysis* 2017; 81:31-44, <https://doi.org/10.1016/j.engfailanal.2017.07.009>.
37. Yazawa E, Takeshita K. Development of measurement device of track irregularity using inertial mid-chord offset method, *Quarterly Report of RTRI* 2002; 43(3):125–130. <https://doi.org/10.2219/rtriq.43.125>